Formation of Ripple Patterns and Dunes by Wind-Blown Sand

Hiraku Nishimori and Noriyuki Ouchi
Department of Physics, Ibaraki University, Mito 310, Japan
(Received 29 September 1992)

Simple models for the formation dynamics of two scales of sand features are proposed. In the simulation of the small scale model, a ripple pattern is spontaneously formed by the saltation of sand grains when the wind force exceeds a critical value. With the large scale model, the dynamics of sand dunes is discussed.

PACS numbers: 81.35.+k, 05.70.Fh, 92.90.+x

On a sand beach, we often find beautiful and various ripple patterns which are made by wind. These ripple patterns emerge when the wind force (shear stress of wind at the sand surface) is within a critical range. The scale of a ripple is of the order of 10 cm. Wind-formed features are much more various at larger scales. Dunes are divided into many classes depending on their size and form.

The formation dynamics of these patterns is essentially complex because of the discreteness of the system on a phenomenological scale; that is, two neighboring sand grains at one instant will not be neighbors at the next instant. In other words, folding and unfolding frequently occur in these systems.

Dynamics of sand patterns was inclusively reported by Bagnold [1]. In [1], based on wide observational and experimental facts, it is reported that the dynamics of sand grains consists of three elementary processes: suspension, saltation, and surface creep. According to [1], saltation is the most important process in the formation dynamics of ripple and other sand features.

Kawamura proposed a linear and continuous model to explain the ripple formation mechanism [2]. Following Bagnold's report [3], Kawamura's linear analysis includes only saltation as the elementary process, but it sufficiently explains how unstable modes are excited in the system. One of his main results is that the wavelength of a ripple increases in proportion to wind force.

In his model, Kawamura allows infinite numbers of unstable bands to coexist independent of wind force. This leaves us two problems: (1) the onset mechanism of a sand ripple at a threshold wind force, and (2) the mechanism for single mode selection. We resolve the first problem and partially understand the second. In addition we make a simple model for sand dunes in order to investigate how the rich variety of sand dune dynamics is realized. Our final purpose is to understand complex dynamics in simple and macroscopically discrete nonlinear systems.

We construct our models from discrete elementary processes, unlike Kawamura's model, in order to realize the discrete nature of the system. As for the elementary processes of dynamics, two of those reported in Bagnold's papers are applied. Our models contain the saltation process like Kawamura's model and, in addition, we take the creeping process into consideration.

We first simulate the model for the small scale feature (sand ripple), and discuss the results using a stability analysis. Next, a model for the larger scale features (sand dunes) is proposed. The former model is named model I, the latter model II.

We start with Model I. The model consists of two elementary processes: saltation and creep. When, under strong wind, a sand grain rolling on a sand surface collides with an obstacle, causing it to be projected into the air, the grain is accelerated by wind, attacks other sand grains on the lee side, and gives them momentum to eject out of the surface. As a result, a chain process is induced in the system. This jumping process is called saltation. Saltation is described as the transfer of a sand grain in the air from one position to another position.

Sand grains may move just along the sand surface without jumping up; this form of movement is called creep. Creep occurs when a sand grain is too heavy to jump up and the wind force is strong enough to move the grain. Creeping on the windward side also occurs by gravity force when the gradient of the sand hill where a grain landed is too steep for it to keep its position.

Our model is a discrete model in space and time with a continuous field variable representing the averaged surface height at each (coarse grained) site. This is a kind of coupled map lattice (CML) model [4]. In the following we first show how the saltation dynamics, and after that creep dynamics, are made.

We first describe the saltation step as

$$\begin{aligned} h_{n'}(x,y) &= h_n(x,y) - q\,, \\ h_{n'}(x+L(h_n(x,y)),y) &= h_n(x+L(h_n(x,y)),y) + q\,, \end{aligned} \tag{1}$$

where $h(x,y)$ is the height of the sand surface at each site (x,y), q is the transferred height of grains moving one (coarse grained) step from one (coarse grained) position (x,y) to the other position $(x+L,y)$ on the lee side. We assume here that q is conserved in this step. $L(h(x,y))$ is the flight length at one saltation. This time step is labeled n. Our complete time step consists of two substeps; one is the saltation step and the other is creep, which will be introduced below. As such we use the

0031-9007/93/71(1)/197(4)$06.00

description n' on the left-hand side of Eq. (1) as the intermediate time step between n and $n+1$. Wind blows in the positive x direction. L depends on many factors in a real system. Using some observational facts and some relations reported in previous papers [1,2,5], the following relation is introduced as a simplest approximation:

$$L = L_0 + b h_n(x,y) . \tag{2}$$

This equation is introduced using a method similar to the one introduced in [2]. Here, L_0 is a control parameter proportional to wind force, i.e., shear stress of wind at the sand surface. The shear stress is known by measuring friction velocity [6] (not wind velocity) of wind at the sand surface. The value of friction velocity is easily obtained from observation data [1,7].

The quantity b is mainly determined from the average wind velocity a grain experiences in flight; however, it is hard to obtain because of the inhomogeneous profile of the wind velocity above the sand surface [3], and the nontrivial trajectory of sand in a saltation step, so b is set constant in our model.

For clarity we should reconfirm that the control parameter is wind force (shear stress of wind) and not wind velocity, which has a complex profile in space.

The physical meaning of this equation is simple, that is, the higher the starting point of a grain, the longer its flight length. In the determination of L, we use two assumptions: (i) We can ignore the topography of the landing point of grains; (ii) we can ignore the information at the takeoff point other than the surface height. The first assumption holds as long as we interpret this model as a kind of mean field model, while, the second fails in the case where we treat the large scale features as follows: Let us think of a grain ejected from a position with an arbitrary height at the windward side of a big sand hill; it will soon land at a higher spot on the same side of the hill independent of the height of the takeoff point. In this large scale case we should care about whether the starting point is the windward side or the lee side of a big hill rather than the height. This will be explained in model II. Oppositely, in the small scale features, we can assume an ejected grain reaches a standard height [8] without being interrupted by the wall of sand hill. As such, the relation of Eq. (2) roughly holds if the features' scale is smaller than, or at most the same as, the scale of saltation. This is just the case for ripple formation.

Next, creep is expressed as

$$h_{n+1}(x,y) = h_{n'}(x,y) + D\left[\frac{1}{6}\sum_{\mathrm{NN}} h_{n'}(x,y) + \frac{1}{12}\sum_{\mathrm{NNN}} h_{n'}(x,y) - h_{n'}(x,y)\right] , \tag{3}$$

where $\sum_{\mathrm{NN}} h_{n'}(x,y)$ describes the summation over the nearest neighboring sites of (x,y) and $\sum_{\mathrm{NNN}} h_{n'}(x,y)$ is the sum over second nearest neighboring sites. The meaning of this process is simple; that is, the local height of a sand hill is relaxed by gravity with a speed proportional to the convexity of the sand surface. D is the rate of relaxation. Though we should have included the asymmetric nature of creep under wind force, we neglected it for the sake of simplicity [9].

The above two processes constitute one unit time step. We repeat the unit step to realize the evolution of the system.

Simulation is performed as follows. Initially the field variable $h(x,y)$ at each site is set randomly with sufficiently small fluctuation around the averaged initial value $h_{\mathrm{standard}}(=0)$. The system size is 100×100. We use periodic boundary conditions in both directions, x and y. This condition is natural when the characteristic wavelength of the ripple is sufficiently shorter than the system size. This condition keeps the total number of grains constant.

Several calculations are done with various sets of control parameters, L_0 and D, with b fixed to 2.0. The results are as follows.

(i) When D and L_0 are appropriately selected, e.g., $D=1.5$ and $L_0=5.0$, starting from an initial pattern with no ripple, the system evolves to form a ripple pattern with a particular wave number [Fig. 1(a)]. (ii) With a fixed $D(=1.5)$, and various L_0, we investigate the steady state of the system. The relation between the wind force L_0 and the selected wavelength is almost linear, as shown in Fig. 2, although below a critical value of L_0 no ripple appears in the system. (iii) Next, simulations are performed with various sets of D and L_0. When D is larger than a critical value which depends on L_0, no ripple pattern is formed in the system. On the other hand, a ripple pattern emerges in the system and remains at steady state, when L_0 is larger than the transient zone in the control parameter space as shown in Fig. 3.

A qualitative explanation for the above results is made by a stability analysis which is based on Kawamura's method. For simplicity, we treat a one-dimensional case. First, we set the height as $h(x,t)=\exp(\sigma t + i\nu x)$. Next, a dynamical equation for $h(x,t)$ is constructed as follows [3]:

$$\frac{dh(x,t)}{dt} = A\left(N(\xi)\frac{d\xi}{dx} - N(x)\right) + D\nabla^2 h(x,t) , \tag{4}$$

where $N(x)$ is the outgoing grain flux from x, and $N(\xi)d\xi/dx$ is the incoming grain flux to x, where $\xi=\xi(x)$ is the x coordinate of the takeoff point of the grains which land at x. A is a scale parameter. Here a one to one correspondence between x and ξ is assumed throughout the relation,

$$x = \xi + L(h(\xi)) = \xi + L_0 + bh(\xi) . \tag{5}$$

The quantity $d\xi/dx$ is the focusing degree of the grains

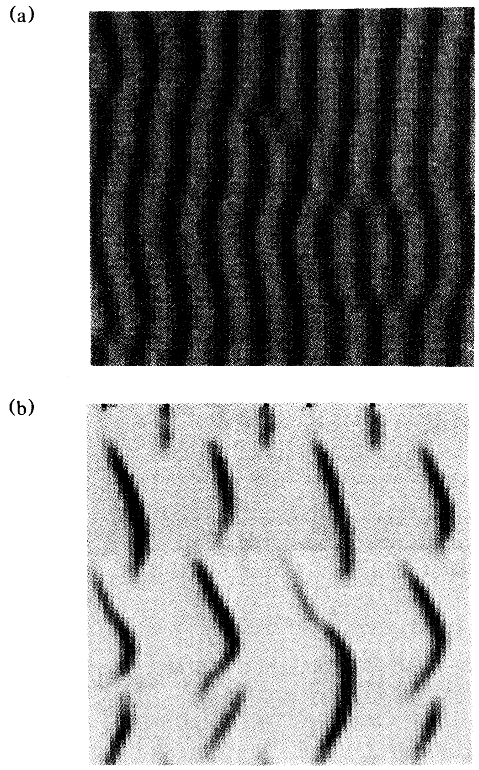

FIG. 1. Snapshots of steady spatial patterns in two limit models. In both systems wind is set to blow from left to right. (a) Sand ripple pattern observed in model I. (b) Barchan dune-like patterns are seen, which move to the right. In (a) deeper shade indicates lower positions in height, while in (b) it indicates higher positions.

jumping from ξ to x. When $d\xi/dx$ is smaller than 1, the grains disperse, while focusing occurs when it is larger than 1. We neglect the case $\partial h(x,t)/\partial x \leq -1/b$ when $d\xi/dx$ diverges or becomes negative and the one to one correspondence of x and ξ is broken.

From Eq. (5), the relation

$$\frac{d\xi}{dx}=\left(1+\frac{dL}{d\xi}\right)^{-1}\cong 1-\frac{dL(h,\xi)}{d\xi} \tag{6}$$

holds.

Inserting the above relation into the right-hand side of Eq. (4), assuming the flux $N(x)$ is independent of position, that is, $N(x)=N(\xi)=N$, and using (2), we get the growth rate of each mode as

$$\tilde{\sigma}\equiv\mathrm{Re}(\sigma)=-ANb\nu\sin(\nu L_0)-D\nu^2 . \tag{7}$$

One can easily know whether $\tilde{\sigma}$ is positive or not by drawing two graphs, $y=-ANb\sin(\nu L_0)$ and $y=D\nu$, as explained in Fig. 4. At a critical value of L_0 depending on D, a contact point between the two graphs appears. This is the onset point of the sand ripple formation. When L_0 increases more, the area with unstable modes

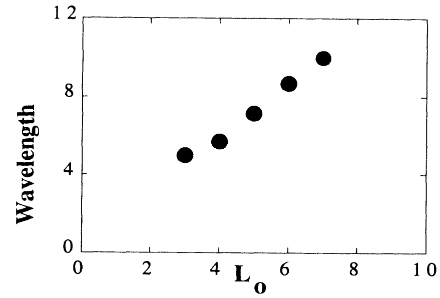

FIG. 2. Wind force L_0 vs selected wavelength of ripple. When L_0 is sufficiently small no ripple is generated.

extends to constitute a band of modes. We have not analyzed what particular mode is selected in this band. It is asserted, at least, the wavelength of the mode with maximum growth rate, $\tilde{\sigma}_{\max}$, increases almost in proportion to L_0 which corresponds to Kawamura's result, Bagnold's observation, and our simulation's result. A similar mechanism works when we change D with L_0 fixed as easily seen from Fig. 4.

Though our theory limits the number of unstable bands to one or a few, the mechanism of single wave selection in these bands is left unsolved.

In the above, we treated the dynamical model for the small scale sand features. We now briefly consider model II for larger scale features. The only differences between model II and model I are the following two points. First, the saltation length of grain started from (x,y) is assumed to be

$$L=L(\nabla\cdot h_n(x,y))=L_0-b\tanh(\nabla\cdot h_n(x,y)) , \tag{8}$$

where L_0 and b are control parameters. The above relation is assumed to apply to the case where the flight length decisively depends on whether the starting point is on the windward side or the lee side of the sand hill. This is the opposite case to the former model (model I). If the hill is much bigger than the scale of saltation, a grain

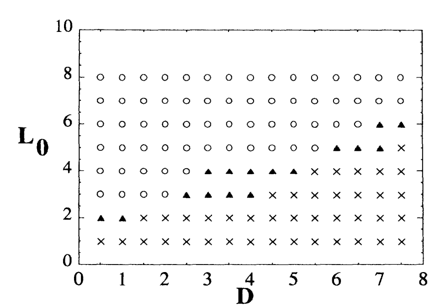

FIG. 3. The phase diagram of steady states in control parameter space. At the positions marked with ○, a ripple appears in the system and occupies the whole system. The × symbols indicate the positions where no ripple pattern is observed to appear. The transient area, where ripple patterns intermittently appear in space and time, is marked with ▲'s.

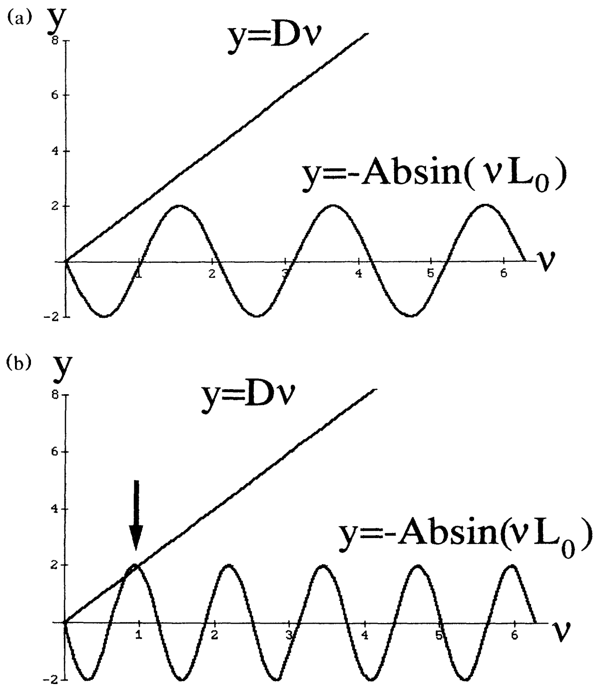

FIG. 4. A schematic explanation for the generation mechanism of sand ripples. When creep rate D is fixed and wind force L_0 is sufficiently large, the growth rate of the wave, $\tilde{\sigma} \equiv \mathrm{Re}(\sigma) = -ANb\nu \sin(\nu L_0) - D\nu^2$, is negative at any wave number ν [(a)]. When L_0 increases to exceed a threshold value the sine curve shrinks to the left and the region in wave number space indicated by the arrow goes unstable [(b)]. This is the same case when D goes below a threshold value with a fixed L_0.

ejected at the windward side of the hill soon clashes into the sand surface near the ejection point, independent of the starting height.

Second, the chance of the surface grains being ejected out by other grains' collision is much larger at the windward side of a hill. So, the transferred height of grains going out by saltation from the position (x,y) per coarse grained unit time period is described as

$$q = q(\nabla \cdot h_n(x,y)) = q_0 + b' \tanh(\nabla h_n(x,y)) , \qquad (9)$$

where q_0 and b' are constants. The patterns we got in this simulation are various in time and space. One of the patterns we got in the simulation is shown in Fig. 1(b), which is similar to a typical form of sand feature named Barchan dune.

A simple qualitative explanation of the rich variety of sand dunes is made by use of stability analysis. The main point is to deform the above model to a linear one. We simplify the flight length as $L = L_0 - b\nabla \cdot h(x,y)$ and set q constant. In this case many bands of modes simultaneously become unstable when D goes below a critical value. We guess this is the origin of the rich variety of large scale features.

To summarize our results, two scales of sand features are treated. The mechanism of the spontaneous emergence of sand ripples and that of wave selection is simulated by model I. Complex dynamics of large scale sand features is reproduced by model II though these are still at the stage of qualitative discussion.

The authors thank Professor Y. Kawada (Kyoto University) for helpful advice. We also thank T. Yanagita (Tokyo Institute for Technology) for stimulating discussions and for the advice on computing. Dr. S. K. Foong is appreciated for a critical reading of this manuscript.

[1] R. A. Bagnold, *The Physics of Blown Sand and Desert Dunes* (Mathuen, London, 1941).

[2] R. Kawamura, Rep. Inst. Sci. Technol., Univ. Tokyo **5**, No. 3/4, 95 (1951).

[3] R. A. Bagnold, Proc. R. Soc. London A **157**, 594 (1936).

[4] K. Kaneko, *Simulating Physics with Coupled Map Lattice,* Dynamics and Statistics of Patterns Vol. 1 (World Scientific, Singapore, 1991); Y. Oono and S. Puri, Phys. Rev. A **38**, 434 (1988).

[5] P. R. Owen, J. Fluid. Mech. **20**, 225 (1964).

[6] Friction velocity u_* is defined as $(\tau_0/\rho)^{1/2}$, where τ_0 is the shear stress of wind at the sand surface and ρ is the density of air. The friction velocity is obtained from the observation date; that is, the time averaged horizontal velocity U at the height z obeys the relation $U = v_*/k \ln(z/z_0)$ where k is known as the Karman universal constant and z_0 is the roughness length of the surface (Ref. [7]).

[7] K. Pye and H. Tsoar, *Aeolian Sand and Sand Dunes* (Unwin Hyman, London, 1990).

[8] Although the flight length also depends on the height of the landing position, here we assume the ejected grain always reaches and lands at the position with an average height, h_{standard}, in space. This is a kind of mean field approximation.

[9] Even if we add an asymmetric term on the right-hand side of Eq. (4), e.g., $\nabla(x,t)$, no qualitative change occurs in the results of our stability analysis.

(a)

(b)

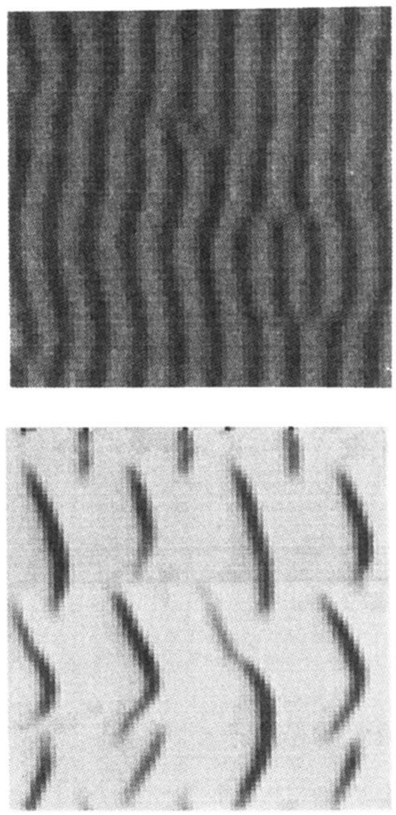

FIG. 1. Snapshots of steady spatial patterns in two limit models. In both systems wind is set to blow from left to right. (a) Sand ripple pattern observed in model I. (b) Barchan dune-like patterns are seen, which move to the right. In (a) deeper shade indicates lower positions in height, while in (b) it indicates higher positions.